Inorganic Chemistry

Article

pubs.acs.org/IC

Simplest Homoleptic Metal-Centered Tetrahedrons, $[M(OH_2)_4]^{2+}$, in 1-Ethyl-3-methylimidazolium Tetrafluoroborate Ionic Liquid (M = Co, Ni, Cu)

Koichiro Takao,*[†] Yurina Tone,[†] Christoph Hennig,[‡] Shohei Inoue,[†] and Taro Tsubomura[†]

[†]Department of Materials and Life Science, Seikei Univeristy, 3-3-1 Kichijoji-kitamachi, Musashino-shi 180-8633 Tokyo, Japan

[‡]Institute of Resource Ecology, Helmholtz-Zentrum Dresden-Rossendorf, P.O. Box 51 01 19, 01314 Dresden, Germany

Supporting Information

ABSTRACT: Dissolution of a tetrafluoroborate or perchlorate salt of $[M(OH_2)_6]^{2+}$ (M = Co, Ni, Cu) in 1-ethyl-3-methylimidazolium tetraluforoborate ionic liquid ([emim]BF_4) results in significant solvatochromism and increasing intensity of color. These observations arise from partial dehydration from the octahedral $[M(OH_2)_6]^{2+}$ and formation of the tetrahedral $[M(OH_2)_4]^{2+}$. This reaction was monitored by the intense absorption band due to the d−d transition in the UV−vis absorption spectrum. The EXAFS investigation clarified the coordination structures around M^{2+} {$[Co(OH_2)_4]^{2+}$, R(Co−O) = 2.17 Å, N = 4.2; $[Cu(OH_2)_4]^{2+}$, R(Cu−O) = 2.09 Å, N = 3.8}. ^{1}H and ^{19}F NMR study suggested that both $[emim]^+$ and BF_4^- are randomly arranged in the second-coordination sphere of $[M(OH_2)_4]^{2+}$.

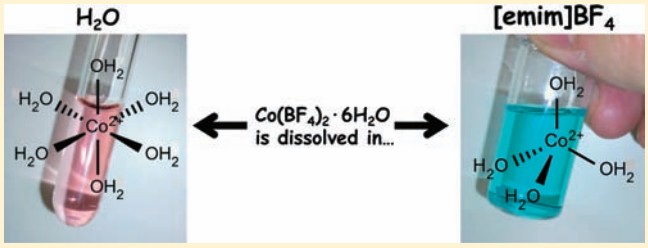

INTRODUCTION

Ionic liquids (ILs) consist of only molecular ions and possess unique characteristics, for instance, a low melting point, very low volatility, high conductivity, and a wide electrochemical potential window. Because of these properties, ILs are regarded as alternative media in various fields, e.g., organic synthesis,[1] electrochemical devices,[2] and nuclear engineering.[3]

Whole aspects on coordination and solution chemistry of metal ions (M^{n+}) in ILs are of great interest, not only in the fundamental science but also for the multidisciplinary applications.[1−4] Because such a medium comprises only completely dissociated molecular cation and anion, a strong ionic atmosphere is formed in this solvent. Furthermore, the anionic species of ILs are usually noncoordinating to M^{n+} (e.g., BF_4^- and PF_6^-) or very weakly Lewis basic (e.g., $R_fSO_3^-$ and $(R_fSO_2)_2N^-$). On this basis, we wondered if a positively charged metal ion (M^{n+}) is able to be present in an IL as a naked ion without any solvation in the first-coordination sphere or appears at least as a less-solvated species. In the former time, pentahydrated uranyl(VI) ion, $UO_2(OH_2)_5^{2+}$, was dissolved in 1-butyl-3-methylimidazolium nonafluorobutanesulfonate ([bmim]NfO, Chart 1) IL, and dehydration from UO_2^{2+} was investigated.[5] As a result, the water molecules solvated to UO_2^{2+} were removed from the first coordination sphere by heating under vacuum. A combined study of UV−vis, Raman, and NMR suggested that UO_2^{2+} is present as the naked cation after the dehydration.

To our best knowledge, the dehydration without successive insertion of any specific ligands has not been known for any other homoleptic aqua complexes, $[M(OH_2)_m]^{n+}$ so far. Such a reaction is, however, not necessarily limited to UO_2^{2+}. If this is also the case for other M^{n+} such as transition metals, the metal complex preparation would no longer suffer from competition between solvation and entering ligand(s). Therefore, a new strategy to synthesize functionalized metal complexes superior to the HSAB principle could be provided. As a first step to develop this chemistry in ILs, we started from several 3d transition metal ions: Co^{2+}, Ni^{2+}, and Cu^{2+}.

Chart 1

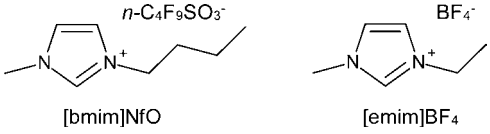

RESULTS AND DISCUSSION

Tetrafluoroborate or perchlorate salts of 3d-metal hexahydrated cations $[Co(OH_2)_6]^{2+}$, $[Ni(OH_2)_6]^{2+}$, and $[Cu(OH_2)_6]^{2+}$ were dissolved in H_2O and 1-ethyl-3-methylimidazolium tetrafluoroborate ([emim]BF_4, Chart 1).[6] The dissolution of the M^{2+} salts in the latter solvent was accelerated by heating under reduced pressure. During this process, vigorous evolution of water vapor was detected. Photographs of these solutions are displayed in Figure 1. For each M^{2+}, the significant change and increasing intensity in color from the aqueous solution to

Received: February 15, 2012
Published: March 23, 2012

   dx.doi.org/10.1021/ic3003433 | Inorg. Chem. 2012, 51, 4850−4854

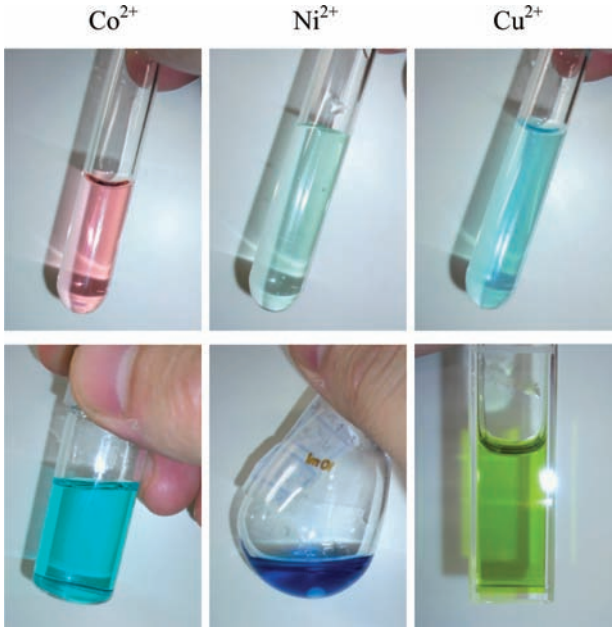

Figure 1. Photographs of several 3d transition metal ions in H_2O (top) and [emim]BF_4 (bottom).

[emim]BF_4 were observed; i.e., Co^{2+}, pink (aq) → sky blue ([emim]BF_4); Ni^{2+}, pale green (aq) → navy blue ([emim]-BF_4); Cu^{2+}, pale blue (aq) → greenish yellow ([emim]BF_4). Such a remarkable solvatochromism clearly indicates that the structure of the first-coordination sphere around M^{2+} is completely different from that in aqueous solution, where M^{2+} occurs in octahedral coordination as $[M(OH_2)_6]^{2+}$. It is noteworthy that the only possible ligand in [emim]BF_4 is H_2O originating from the hydrated water in the starting salt because the anionic component of the IL used here, BF_4^-, is regarded as a noncoordinating anion (though there is an exception[7]). Such color change could arise from the modification of the hydrated structure around M^{2+} in [emim]BF_4.

A UV−vis absorption spectrum of Co^{2+} in [emim]BF_4 is shown in Figure 2 together with those of the same Co^{2+} salt dissolved in H_2O, dimethyl sulfoxide (DMSO), and hexamethylphosphoric triamide (HMPA). Purple and blue solutions were obtained for DMSO and HMPA, respectively. Weak absorption bands of the aqueous and DMSO solutions were observed at 510 nm (molar absorptivity, ε = 5.0 $M^{-1}\cdot cm^{-1}$) and 540 nm (ε = 12 $M^{-1}\cdot cm^{-1}$), respectively, which arise from the characteristic d−d transition strictly electric-dipole forbidden in O_h symmetry of $[Co(L)_6]^{2+}$ (L = H_2O, DMSO).[8] In contrast, the [emim]BF_4 and HMPA solutions show much stronger bands at around 600−700 nm with ε = 550−570 $M^{-1}\cdot cm^{-1}$ at the peak maxima. Break of the Laporte forbiddenness is evidence for the lack of an inversion center at the Co^{2+} center in [emim]BF_4 and HMPA. The most plausible structure around Co^{2+} in these solutions is T_d $[Co(L)_4]^{2+}$ (L = H_2O, HMPA). The well-resolved fine structure of the absorption band in [emim]BF_4 also suggests that the occurring Co^{2+} species forms a simple coordination like $[Co(OH_2)_4]^{2+}$. The similarly structured spectrum is known for the tetrachloro complex, $[CoCl_4]^{2-}$, which is also homoleptically four-coordinated in T_d geometry.[8]

From a concentrated HMPA solution of $Co(BF_4)_2\cdot 6H_2O$, blue platelet crystals deposited. The elemental analysis identified this compound as $[Co(HMPA)_4](BF_4)_2$.[9] Its molecular and crystal structures were determined by single crystal X-ray diffraction. As expected, Co^{2+} is surrounded by four HMPA molecules with T_d symmetry as shown in Figure S1 of the Supporting Information.[10] Although the weighted and unweighted agreement factors are relatively large, no significant residual electron density was found in the final Fourier map ($\Delta\rho_{max}$ = 1.030 $e^-\cdot Å^{-3}$, $\Delta\rho_{min}$ = −0.730 $e^-\cdot Å^{-3}$). The uncertainty may arise from the largely disordered F atoms of BF_4^- as a counteranion. The Co−O interatomic distances are in the range of 1.938−1.953 Å (mean 1.95 Å) and are similar to another Co^{2+} complex in T_d symmetry.[10] Although the O−Co−O bond angle is scattering widely from 104.0° to 116.7°, the mean value is 109.5°, which is ideal for the regular tetrahedron.

The Co^{2+} species occurring in [emim]BF_4 is supposed to be an aqua complex with T_d symmetry because of the similarities in the solution color and the UV−vis absorption spectrum to the HMPA system. For the moment, our trial to isolate a crystalline Co^{2+} salt from [emim]BF_4 is not successful. Instead, we measured a Co K-edge extended X-ray absorption fine structure (EXAFS) spectrum[12] to extract the structural information of Co^{2+} in [emim]BF_4. As shown in Figure 3, a

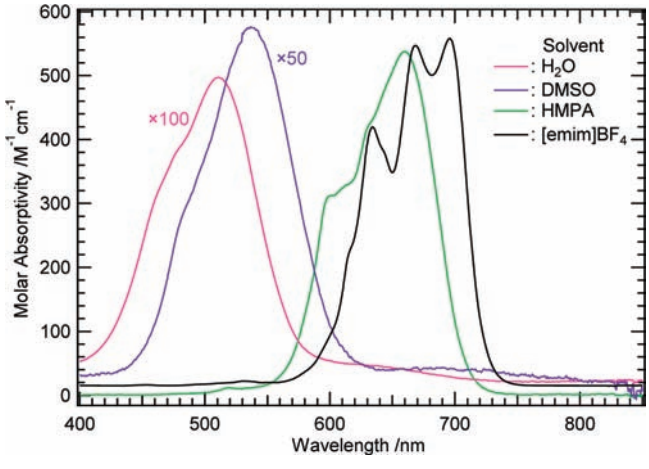

Figure 2. UV−vis absorption spectra of H_2O, DMSO, HMPA, and [emim]BF_4 solutions dissolving $Co(BF_4)_2\cdot 6H_2O$. The ε axis of the spectra of H_2O and DMSO solutions were magnified by multiplying appropriate factors (×100 and ×50, respectively).

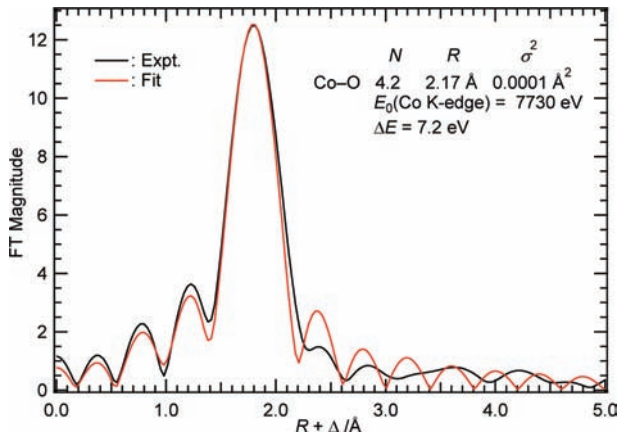

Figure 3. Fourier transformed k^3-weighted Co K-edge EXAFS spectrum of Co^{2+} (3.3 × 10^{-2} M) in [emim]BF_4.

dx.doi.org/10.1021/ic3003433 | Inorg. Chem. 2012, 51, 4850−4854

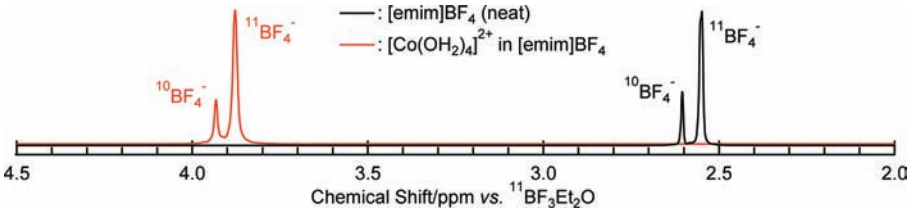

Figure 4. ^{19}F NMR spectra of $[emim]BF_4$ solution in presence and absence of $[Co(OH_2)_4]^{2+}$ (3.3×10^{-2} M) at 295 K.

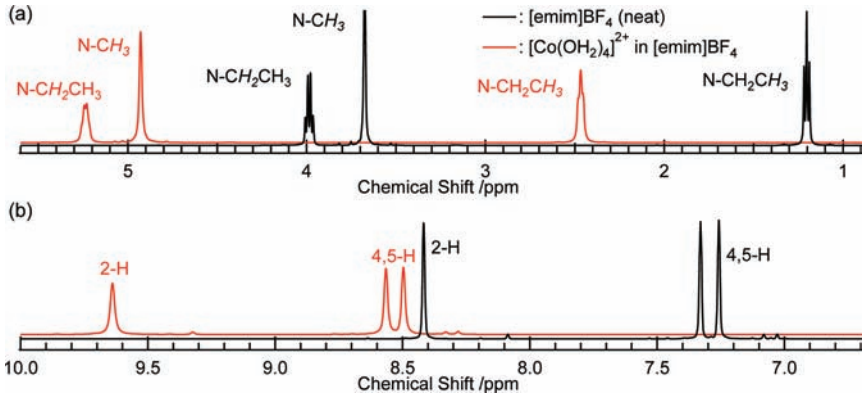

Figure 5. ^1H NMR spectra of $[emim]BF_4$ solution in presence and absence of $[Co(OH_2)_4]^{2+}$ (3.3×10^{-2} M) at 295 K. Chemical shift range: 0.9–5.6 ppm (a) and 6.7–10.0 ppm (b).

single peak at $R + \Delta = 1.8$ Å occurs in the Fourier transformed EXAFS spectrum. The curve fit using a single Co–O shell indicates that Co^{2+} is surrounded by 4.2 O atoms with a Co–O distance of 2.17 Å. The latter is indeed longer than the usual lengths in T_d symmetry (typically 1.95 Å found in $[Co(HMPA)_4]^{2+}$ and ref 10), while closer to, but still slightly longer than, those of O_h $[Co(OH_2)_6]^{2+}$ (2.06–2.14 Å).[12] By combining the EXAFS and UV–vis data, it can be concluded that the T_d $[Co(OH_2)_4]^{2+}$ is formed in $[emim]BF_4$. The other possible geometry for the tetra-aqua complex is square planar (*SP*). However, this geometry is exclusively unlikely because of the lack of an inversion center clarified in the UV–vis absorption spectroscopy (Figure 2) and no significant multiple scattering contribution at twice the $R + \Delta$ of the Co–O distance (Figure 3). Although the X-ray absorption spectrum in the pre-edge region was recorded with a larger energy step (1.0 eV) compared to that of the postedge, the peak at 7709 eV in Figure S2 of the Supporting Information is attributable to the Laporte forbidden electron excitation from 1s to 3d orbital, and its occurrence is also indicative of the absence of the inversion center at Co^{2+}, i.e., T_d geometry of $[Co(OH_2)_4]^{2+}$.

Now a question arises: what drives formation of the T_d Co^{2+} species in HMPA and $[emim]BF_4$? In HMPA, the ligand substitution from the water molecules to the solvent ones surely takes place. The occurrence of the T_d $[Co(HMPA)_4]^{2+}$ is reasonably explained by the steric hindrance between the neighboring bulky HMPA molecules in the complex. In contrast, such a steric demand between the water molecules bound to Co^{2+} cannot be expected. Considering that the strong ionic atmosphere is formed in $[emim]BF_4$, charge density on the molecular surface of a dissolved species would tend to become higher. Thus, a smaller surface area of the dissolved species should be more preferable in such a system. This may explain the decrease in hydration number around Co^{2+} from 6 to 4 and formation of the T_d $[Co(OH_2)_4]^{2+}$ in $[emim]BF_4$.

Solvation in the second-coordination sphere of the T_d $[Co(OH_2)_4]^{2+}$ in $[emim]BF_4$ is also of interest. This tetra-aqua species has seven d-electrons, and results in $e^4t_2^3$ electronic configuration with $S = 3/2$ at the ground state, i.e., paramagnetic. Therefore, ^1H and ^{19}F NMR spectra of $[emim]^+$ and BF_4^- will be affected by this paramagnetism, providing the information of the second-coordination structure around $[Co(OH_2)_4]^{2+}$ in $[emim]BF_4$. The ^{19}F NMR spectrum of $[emim]BF_4$ containing $[Co(OH_2)_4]^{2+}$ (3.3×10^{-2} M) is displayed in Figure 4 together with that of the neat $[emim]BF_4$. As a result, a single pair of ^{19}F signals arising from $^{10}BF_4^-$ and $^{11}BF_4^-$ isotopomers[13] has been observed at 3.88 and 3.93 ppm vs $^{11}BF_3{\cdot}Et_2O$ in the presence of $[Co(OH_2)_4]^{2+}$. This signal pair is significantly shifted downfield by 625 Hz compared to the neat $[emim]BF_4$ (2.55 and 2.60 ppm vs $^{11}BF_3{\cdot}Et_2O$). The former observation implies that the chemical exchange of BF_4^- in the second-coordination sphere with that in bulk is very rapid in the NMR time-scale. The paramagnetic shift ($\Delta\nu$) is regarded to arise only from the pseudocontact shift between BF_4^- and $[Co(OH_2)_4]^{2+}$ because of the poor coordinating character of BF_4^- to M^{n+}. The large paramagnetic shift of the ^{19}F signals of BF_4^- could be reasonable because the positively charged $[Co(OH_2)_4]^{2+}$ attracts the negatively charged BF_4^- by the electrostatic interaction. No remarkable differences in the isotopic shift by $^{10}B/^{11}B$ were detected, i.e., $\Delta\delta = 0.05$ ppm between $^{10}BF_4^-$ and $^{11}BF_4^-$ in the presence and absence of $[Co(OH_2)_4]^{2+}$ in $[emim]BF_4$. Slight line-broadening of the ^{19}F signals (fwhm, +1.6 Hz for $^{11}BF_4^-$; +1.9 Hz for $^{10}BF_4^-$) due to the paramagnetic $[Co(OH_2)_4]^{2+}$ was observed. It is also noteworthy that any other ^{19}F signals were not detected, implying that BF_4^- is not hydrolyzed in this solution.

The ^1H NMR spectra of the same solution were also recorded as shown in Figure 5. The paramagnetic downfield shifts similar to ^{19}F (Figure 4) were also recognized for all the signals of $[emim]^+$. The magnitude of the shift of each signal is ranging 611–632 Hz, which is almost the same as that of BF_4^-

dx.doi.org/10.1021/ic3003433 | *Inorg. Chem.* 2012, 51, 4850–4854

in Figure 4. This is somewhat surprising because strong electrostatic repulsion was expected between $[Co(OH_2)_4]^{2+}$ and $[emim]^+$, and therefore, the tetra-aqua complex was predicted to be exclusively surrounded by BF_4^- rather than $[emim]^+$. The actual result implies that $[emim]^+$ also enters the second-coordination sphere of $[Co(OH_2)_4]^{2+}$ with the similar lifetime to stay there because $\Delta\nu$ rapidly decreases as a function with the third power of the distance from the paramagnetic Co^{2+} center as long as the lifetimes of the cation and anion in the second-coordination sphere are the same.[14] Therefore, one can imagine that both $[emim]^+$ and BF_4^- are randomly arranged around $[Co(OH_2)_4]^{2+}$.

Cu^{2+} in $[emim]BF_4$ was also examined by the same experiments. The obtained UV−vis, EXAFS and NMR spectra are shown in the Supporting Information. The intense greenish-yellow color of Cu^{2+} in $[emim]BF_4$ results from a strong absorption at 400 nm with ε = 1580 $M^{-1}\cdot cm^{-1}$, while a weaker and broader band centered at 900 nm (ε = 190 $M^{-1}\cdot cm^{-1}$) is also lying (Figure S3 of Supporting Information).[15] Furthermore, from the Cu K-edge EXAFS spectrum, it was suggested that 3.8 O atoms bind to Cu^{2+} with a distance 2.09 Å in $[emim]BF_4$ (Figure S4 of Supporting Information). The pre-edge feature was detected at 8977 eV (Figure S2 of Supporting Information), indicating the lack of the inversion center at Cu^{2+}. By comparing these findings with the much weaker blue color of $[Cu(OH_2)_6]^{2+}$ in aqueous solution (λ_{max} = 800 nm, ε = 10 $M^{-1}\cdot cm^{-1}$), it can be concluded that the T_d $[Cu(OH_2)_4]^{2+}$ is also formed in $[emim]BF_4$. In line with the former reports on $[CuCl_4]^{2-}$,[16] the $[Cu(OH_2)_4]^{2+}$ tetrahedron in $[emim]BF_4$ might be somewhat flattened. The four-coordinated Cu^{2+} usually prefers the *SP* geometry because of the Jahn−Teller effect in d^9 electronic configuration.[8] In contrast, $[Cu(OH_2)_4]^{2+}$ in $[emim]BF_4$ tends to be in the T_d coordination despite the unlikelihood of the considerable steric crowding in the first coordination sphere. The preferred T_d form rather than *SP* is convincing from a viewpoint of uniform charge distribution around $[Cu(OH_2)_4]^{2+}$ immersed in the strong ionic atmosphere of $[emim]BF_4$. The paramagnetic shift for BF_4^- (108 Hz, Figure S5 of Supporting Information) is not very different from those for $[emim]^+$ (84−105 Hz, Figure S6 of Supporting Information), implying the random arrangement of $[emim]^+$ and BF_4^- in the second-coordination sphere of $[Cu(OH_2)_4]^{2+}$.

The study on Ni^{2+} in $[emim]BF_4$ was just started, and only the significant solvatochromism and color intensification displayed in Figure 1 were confirmed at the moment. By combining this fact and the general trend found in Co^{2+} and Cu^{2+}, a similar T_d $[Ni(OH_2)_4]^{2+}$ can be reasonably expected to occur in $[emim]BF_4$. This hypothesis is also in line with the former isolation of blue-colored T_d Ni^{2+} complexes, $NiX_2(OAsPh_3)_2$ (X = Cl, Br).[17]

CONCLUSIONS

In this study, we investigated the solvation of Co^{2+}, Ni^{2+}, and Cu^{2+} in $[emim]BF_4$ ionic liquid. In all the cases of M^{2+} studied, the starting hexahydrated M^{2+} exhausts 2 water molecules in $[emim]BF_4$, resulting in the tetrahedrally coordinated $[M(OH_2)_4]^{2+}$ as monitored by the significant solvatochromism and increasing intensity of the color. Although other homoleptic tetrahedral species have already been known (e.g., $[CoCl_4]^{2+}$),[8] the tetra-aqua 3d metal complexes in T_d symmetry are most fundamental in the coordination chemistry and observed for the first time in the present study. Trials for further dehydration employing physical and/or chemical techniques are in progress now. Our tentative goal on this chemistry is to ascertain the ultimately dehydrated state of M^{n+} in ILs.

EXPERIMENTAL SECTION

1-Ethyl-3-methylimidazolium tetrafluoroborate, $[emim]BF_4$, was prepared and purified by the reported method.[6] All the M^{2+} salts ($Co(BF_4)_2\cdot 6H_2O$, $Ni(ClO_4)_2\cdot 6H_2O$, and $Cu(BF_4)_2\cdot 6H_2O$) and solvents (DMSO and HMPA) were commercially available and used as received. The deionized water was used to prepare the aqueous samples.

UV−vis absorption spectra were recorded by SHIMADZU UV-3100PC spectrophotometer. The optical path length of the used conventional quartz cell was 1 cm.

The EXAFS spectra were measured at Rossendorf Beamline BM20 in the European Synchrotron Radiation Facility.[11] A Si(111) double-crystal monochromator was employed in channel-cut mode to monochromatize the white X-ray from the synchrotron. Co and Cu K-edge X-ray absorption spectra of the $[emim]BF_4$ solutions confined in polyethylene tubes (1 mm inner diameter) were recorded in fluorescence mode using 13-element Ge solid state detector (Canberra). The threshold energy values $E_{k=0}$ of Co and Cu K-edge were arbitrarily defined at 7730 and 9000 eV, respectively. The X-ray absorption spectra of Co and Cu were measured 10 times and 3 times, respectively, and merged. The obtained spectra were processed using Athena for background removal and the extraction of EXAFS spectra and Artemis for the EXAFS curve fit.[18] The curve fit was performed in the *R*-space, using phases and amplitude calculated by *FEFF* 8.20.[19] A single shell of M−O (M = Co, Cu) was assumed in the fit. The amplitude decay factor S_0^2 was fixed at 0.9.

The NMR experiments were performed by using a JEOL ECA-500 NMR spectrometer. As an external lock solvent, a glass capillary filled with D_2O solution dissolving 0.2 wt % 3-(trimethylsilyl)propionic-2,2,3,3-d_4 acid sodium salt (TSP-d_4) was inserted in each NMR sample tube. In all the ^1H NMR spectra reported here a signal from the trimethylsilyl group of TSP-d_4 in the capillary was used as an external reference for the chemical shift. The ^{19}F NMR spectra were recorded versus a ^{19}F signal of boron-11 trifluoride diethyl etherate (BF_3Et_2O) external reference.

A single crystal X-ray diffraction measurement for $[Co(HMPA)_4](BF_4)_2$ was performed by the following procedure. The single crystal was mounted in a cryo-loop together with Paratone-N oil and placed under a low-temperature nitrogen gas stream at 123 K. Intensity data were collected using a CCD detector in a Rigaku Saturn70 diffractometer with graphite-monochromated Mo Kα radiation (λ = 0.71073 Å). The structure was solved by SHELXS97[20] and expanded using Fourier techniques. All non-hydrogen atoms were anisotropically refined using SHELXL-97.[20] Each hydrogen atom included in the structure was refined as riding on its parent carbon atom with $U_{iso}(H) = 1.2U_{eq}(C)$. The final cycle of full-matrix least-squares refinement on F^2 was based on observed reflections and parameters and converged with unweighted and weighted agreement factors, *R* and *wR*. All computations were performed with the CrystalStructure crystallographic software package.[21] Crystallographic data for $[Co(HMPA)_4](BF_4)_2$: $C_{24}H_{72}B_2CoF_8N_{12}O_4P_4$; M_W = 949.35; 0.40 × 0.54 × 0.48 mm^3; orthorhombic; *Pbca*; *a* = 20.74(3), *b* = 17.03(3), *c* = 25.84(4) Å; *V* = 9127(21) $Å^3$; *Z* = 8; ρ_{calcd} = 1.382 $Mg\cdot m^{-3}$; μ = 0.593 mm^{-1}; *T* = 123 K; 76 755 reflections; 10 183 independent; R_{int} = 0.0564; R_1 = 0.1325 ($[F^2 > 2\sigma(F^2)]$); wR_2 = 0.2939 (all data); GOF = 1.320; Θ = 3.03 to 27.48°; $\Delta\rho_{max}$ = 1.030; $\Delta\rho_{min}$ = −0.730 $e^-\cdot Å^{-3}$. CCDC 852891 contains the supplementary crystallographic data for this Article. These data can be obtained free of charge from www.ccdc.cam.ac.uk/data_request/cif or the Supporting Information of this Article.

All the analytical experiments except for the single crystal X-ray diffraction were performed at 295 ± 1 K.

dx.doi.org/10.1021/ic3003433 | *Inorg. Chem.* 2012, 51, 4850−4854

■ ASSOCIATED CONTENT

Supporting Information

ORTEP drawing of $[Co(HMPA)_4]^{2+}$, NMR, UV−vis absorption, and EXAFS spectra of $[emim]BF_4$ solutions containing Cu^{2+} and crystallographic information file for $[Co(HMPA)_4](BF_4)_2$. This material is available free of charge via the Internet at http://pubs.acs.org.

■ AUTHOR INFORMATION

Corresponding Author

*E-mail: k.takao@st.seikei.ac.jp.

Notes

The authors declare no competing financial interest.

■ ACKNOWLEDGMENTS

This work was supported by a research grant from Seikei University.

■ REFERENCES

(1) (a) Olivier-Bourbigou, H.; Magna, L. *J. Mol. Catal. A: Chem.* **2002**, *182*−*183*, 419−437. (b) Earle, M. J.; Seddon, K. R. *Pure Appl. Chem.* **2000**, *72*, 1391−1398. (c) Wasserscheid, P.; Keim, W. *Angew. Chem., Int. Ed.* **2000**, *39*, 3772−3789. (d) Welton, T. *Chem. Rev.* **1999**, *99*, 2071−2083. (e) Dupont, J.; De Souza, R. F.; Suarez, P. A. Z. *Chem. Rev.* **2002**, *102*, 3667−3692.

(2) Bonhôte, P.; Dias, A.-P.; Armand, M.; Papageorgiou, N.; Kalyanasundaram, K.; Grätzel, M. *Inorg. Chem.* **1996**, *35*, 1168−1178; *Inorg. Chem.* **1998**, *37*, 166.

(3) (a) Bradley, A. E.; Hatter, J. E.; Nieuwenhuyzen, M.; Pitner, W. R.; Seddon, K. R.; Thied, R. C. *Inorg. Chem.* **2002**, *41*, 1692−1694. (b) Bradley, A. E.; Hardacre, C.; Nieuwenhuyzen, M.; Pitner, W. R.; Sanders, D.; Seddon, K. R.; Thied, R. C. *Inorg. Chem.* **2004**, *43*, 2503−2514. (c) Visser, A. E.; Jensen, M. P.; Laszak, I.; Nash, K. L.; Choppin, G. R.; Rogers, R. D. *Inorg. Chem.* **2003**, *42*, 2197−2199. (d) Chaumont, A.; Wipff, G. *Phys. Chem. Chem. Phys.* **2006**, *8*, 494−502. (e) Ouadi, A.; Klimchuk, O.; Gaillard, C.; Billard, I. *Green Chem.* **2007**, *9*, 1160−1162. (f) Ogura, T.; Takao, K.; Sasaki, K.; Arai, T.; Ikeda, Y. *Inorg. Chem.* **2011**, *50*, 10525−10527.

(4) For example, (a) Binnemans, K. *Chem. Rev.* **2007**, *107*, 2592−2614. (b) Cocalia, V. A.; Gutowski, K. E.; Rogers, R. D. *Coord. Chem. Rev.* **2006**, *250*, 755−764.

(5) Mizuoka (Takao), K.; Ikeda, Y. *Prog. Nucl. Energy* **2005**, *47*, 426−433.

(6) Takao, K.; Ikeda, Y. *Chem. Lett.* **2008**, *37*, 682−683.

(7) Honeychuck, R. V.; Hersh, W. H. *Inorg. Chem.* **1989**, *28*, 2869−2886.

(8) Figgis, B. N.; Hitchman, M. A. *Ligand Field Theory and Its Applications*; Wiley-VCH: New York, 2000.

(9) Elemental analysis $[Co(HMPA)_4](BF_4)_2$, $C_{24}H_{72}B_2CoF_8N_{12}O_4P_4$, Calcd: C, 30.36; H, 7.64; N, 17.71. Found: C, 30.78; H, 7.40; N, 17.34.

(10) Dobrzynska, D.; Lis, T.; Wozniak, J. *Acta Crystallogr.* **2006**, *E62*, m1006−m1008.

(11) Reich, T.; Bernhard, G.; Geipel, G.; Funke, H.; Hennig, C.; Rossberg, A.; Matz, W.; Schell, N.; Nitsche, H. *Radiochim. Acta* **2000**, *88*, 633−637.

(12) Lee, U.; Jung, Y.-H.; Joo, H.-C.; Park, K.-M. *Acta Crystallogr.* **2003**, *E59*, m421−424.

(13) (a) Kuhlmann, K.; Grant, D. M. *J. Phys. Chem.* **1964**, *68*, 3208−3213. (b) Harris, R. K.; Mann, B. E. *NMR and the Periodic Table*; Academic Press, Inc.: London, U.K., 1978; p 99.

(14) La Mar, G. N.; De Horrocks, W., Jr.; Holm, R. H. *NMR of Paramagnetic Molecules Principles and Applications*; Academic Press, Inc.: New York, 1973; p 377.

(15) The absorption spectrum at $\lambda > 1100$ nm was not recorded because of strong absorption by $[emim]BF_4$.

(16) (a) Harlow, R. L.; Wells, W. J. III; Watt, G. W.; Simonsen, S. H. *Inorg. Chem.* **1974**, *13*, 2106−2111. (b) Willett, R. D.; Haugen, J. A.; Lebsack, J.; Morrey, J. *Inorg. Chem.* **1974**, *13*, 2510−2513. (c) Riley, M. J.; Neill, D.; Bernhardt, P. V.; Byriel, K. A.; Kennard, C. H. L. *Inorg. Chem.* **1998**, *37*, 3635−3639. (d) Haddad, S.; Willett, R. D. *Inorg. Chem.* **2001**, *40*, 2457−2460.

(17) Goodgame, D. M. L.; Cotton, F. A. *J. Am. Chem. Soc.* **1960**, *82*, 5774−5776.

(18) Ravel, B; Newville, M. *J. Synchrotron Radiat.* **2005**, *12*, 537−541.

(19) Ankudinov, A. L.; Ravel, B.; Rehr, J. J.; Conradson, S. D. *Phys. Rev. B* **1998**, *58*, 7565−7576.

(20) Sheldrick, G. M. *Acta Crystallogr.* **2008**, *A64*, 112−122.

(21) *CrystalStructure 4.0*, Crystal Structure Analysis Package; Rigaku Corporation: Tokyo, Japan, 2010.